

## Phase Distortion Correction for See-Through-The-Wall Imaging Radar

Jay A. Marble and Alfred O. Hero  
University of Michigan - Dept. of Electrical Engineering and Computer Science  
Ann Arbor, Michigan 48109-2122

### ABSTRACT

See Through The Wall (STTW) applications have become of high importance to law enforcement, homeland security and defense needs. In this work surface penetrating radar is simulated using basic physical principles of radar propagation. Wavenumber migration is employed to form 2D images of objects found behind a wall. It is shown that this technique cannot properly image with the wall present because of an unknown phase delay experienced by the electromagnetic waves as they pass through the wall. Two approaches are taken to estimate this phase by looking at the direct backscatter signal from the wall. The first is a dual phase approach, which uses a non-parametric technique to find the phase at every frequency. The second method is a dual frequency approach. The two frequencies are close enough together that the reflection coefficients are approximately equal. This approximation allows for more observations than unknown parameters. The surface reflection coefficient, back wall coefficient, and phase are simultaneously determined using an iterative, non-linear (Newton-Raphson) successive approximation algorithm. Comparisons are performed for a simple scenario of three point scatterers with and without phase correction.

### 1. OVERVIEW

Approximations and simulations are used in this work to gain physical insight into the spatial signatures produced by objects observed by surface penetrating radar. The radar system is a receiver/transmitter pair that scans along the outside of a building. The returns can be used to produce an image (slice) of the interior of the room.

The imaging approach used in this work is wavenumber migration. It was first introduced in synthetic aperture radar imaging by [1]. The method was first developed for seismology [2,3]. The principal contribution of this paper is the application of this approach to See-Through-The-Wall radar imaging.

The wavenumber migration algorithm works as follows. The 2D complex spectrum of the image is constructed by properly reformatting the plane waves received by the radar system. The reformatting requires exact knowledge of the phase of the propagating waves. When a wall of unknown thickness and permittivity is introduced, the algorithm can no longer focus the image because the wall imposes an unknown delay on each plane wave due to the

decreased and unknown propagation speed within the wall. To properly reformat the waves, the wavenumber migrator must know the bulk effect of these two parameters (unknown permittivity and unknown thickness) and remove that phase delay from the recorded data.

Adding to the complication of this problem is the fact that the reflection coefficients of the wall are unknown. In this work we will assume that the radar return from the wall is composed of a reflection from the front surface and a reflection from the back surface. These two returns sum together to form a signal in noise with two unknown reflection coefficients and one unknown phase. Due to the non-linear nature in which these three parameters manifest themselves in the returned signal, some assumptions will have to be made in order to estimate them. Two approaches can be considered.

The first approach assumes that the reflection from the wall surface has been removed by some other means. This greatly simplifies the problem and allows for the back of the wall reflection coefficient and the phase at all required frequencies to be removed using a sine and cosine or dual phase technique. This approach is, therefore, a non-parametric approach that estimates the phase at all frequencies. In practice, it may be a significant technical challenge to eliminate the surface reflection contribution as required by this method. Therefore, a second technique is proposed.

The second technique is a dual frequency approach. Here it is assumed that the frequencies are close enough together so that the reflection coefficients of the wall are nearly constant in frequency. The phase unknown is reduced to its fundamental unknown part, which is the product of the wall thickness ( $\tau$ ) and the square root of the wall permittivity ( $\epsilon_2$ ). By relying on a cross-demodulated signal (that is a transmitted cosine mixed with a sine on receive) the wall return is naturally rejected. Two separate soundings are made at the two frequencies. After the cross-demodulation the reflection coefficient of the back of the wall and the phase parameter are non-linearly coupled within the signal. A non-linear iterative maximum likelihood estimation approach is used to separate these two parameters via the Newton-Raphson algorithm. When this algorithm converges, it provides a parametric estimate of the thickness-permittivity-squareroot product. With this estimated parameter, the phase delay for any frequency of interest can be predicted.

We adopt a physical optics model for electromagnetic wave propagation for a simple environment consisting of three point scatterers placed behind the wall. These simulations are used to show the result of correcting the imaging signals with the estimated phase. Images produced without phase correction are also provided to demonstrate the need for correcting unknown phase distortion.

## 2. POINT TARGET SIMULATIONS

The simulation consists of a stepped frequency radar generating frequencies from 500MHz to 2.5GHz with equal steps, a homogeneous wall, and three point scatterers. Figure 2.1 shows the point scatterer arrangement. The radar is pointed directly at the wall. The imaging algorithm operates on a measurement of radar backscatter at 256 frequencies observed at 201 locations parallel to the wall. We define a local coordinate system (also shown in Figure 2.1) at a specified center of the generated image.

We employ a physical optics model of radar wave propagation through the medium. Specifically, the radar rf field is mathematically modeled as plane waves. The reflections from the wall and back of the wall are governed by Fresnel Reflection Coefficients, which are valid

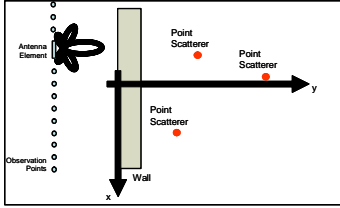


Figure 2.1: Three Point Scatterer Simulations

for time harmonic plane waves. For this work, refraction effects predicted by Snell's Law have been ignored for simplicity. Snell's Law predicts that the waves will be bent as they enter and leave the non-free space media. In this paper we neglect this effect and assume that the waves travel straight through the wall regardless of angle of incidence.

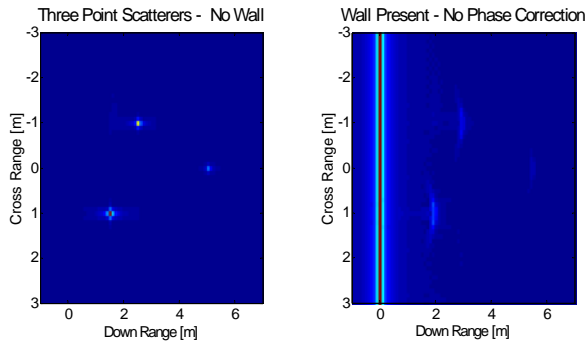


Figure 2.2: Point Simulation – (left) No Wall (right) Wall Inserted

The imaging algorithm used to reconstruct the image of the three point scatterers is wavenumber migration. This method transforms

the received signals into the 2D frequency space and manipulates the phase of each wavenumber. Interpolations (i.e. resampling) is also applied to format the data properly in preparation for a 2D inverse FFT. With correct interpolation and phasing, the energy of point scatterers become *focused* [4]. This can be seen in the free space (no wall) simulation shown in Figure 2.2. The 3 point scatterers are clearly well focused into point targets in this simulation. Their amplitudes can be seen to fade for targets that are further away from the wall. This is due to the  $1/r^2$  spherical spreading of the energy in the transmitted wave. In these simulations the radar is just 6 meters from the farthest point scatterer. At these distances beam divergence loss of the transmit energy can't really be ignored. The point targets have the same radar cross section (10dB).

Figure 2.3 shows the motivation of this work. When the wall is inserted between the radar and the point scatterers, the imaging algorithm cannot focus the points. This is due to an unknown phase factor that is now present in the data stream. A simplified model of the observations is given by Equation 2.1.

$$y(f, x) = a_p(f) e^{-j\phi_p(f, x)} a_w(f) e^{-j\phi_w(f, x)} \rho_n e^{-j\phi_n} \quad \text{Equation 2.1}$$

The amplitude and phase labeled  $a_p$  and  $\phi_p$  are due to the free space propagation between the radar and the  $n^{\text{th}}$  point scatterer. The complex reflectivity of the scatterer is given in amplitude by  $\rho_n$  and  $\phi_n$ . The effect of the wall is to produce an attenuation and phase (both of which are unknown) given by  $a_w$  and  $\phi_w$ .

Under this model the wall acts as a filter that attenuates some of the incident energy. If this is a function of frequency, it would have to be estimated, if the goal is to reconstruct the true reflectivity of all the pixels in the image. On the other hand, if the goal is to reconstruct the location of the scatterers in the image, the amplitude attenuation can be ignored [4]. Of course, in the presence of noise or interference the power transmitted by the radar must be enough to provide a usable signal-to-noise ratio of the received amplitudes. The effect of the phase  $\phi_w$  is to distort the reconstructed image. Hence the phase must be estimated explicitly prior to image reconstruction. Note that the wall parameters are the same for all simulations in this work: relative permittivity of the wall is 10 and it is 0.2 m thick.

## 3. WALL PHASE DETERMINATION AND CORRECTION

Two methods are proposed here for determining the phase caused by a wall of unknown permittivity and unknown thickness. Both methods utilize a pulsed radar. The pulses contain a cosine waveform with just 1 frequency that lasts 100μsec. The return signal is assumed to be a superposition of two cosine functions. The first is from the surface of the wall and the second is from the back of the wall. Equation 3.1 shows the expected return.

$$r(t) = a_0 \cos(\omega t - \theta) + a_1 \cos(\omega t - \theta - \phi) + n(t)$$

$$\theta = \frac{4\pi f}{c} h \quad \phi = \frac{4\pi f}{c} \tau \sqrt{\epsilon_2} \quad \text{Equations 3.1}$$

The  $\theta$  parameter is the expected phase delay due to the waveform propagating to the wall surface and back to the radar. It is reasonable to expect this value to be known. The  $\phi$  parameter on the other hand, contains the  $\tau\sqrt{\epsilon_2}$  value that is unknown. The  $a_0$  and  $a_1$  values are related to the reflection coefficients of the front and back wall surface. The noise  $n(t)$  is an unknown, performance limiting factor.

### 3.1 Dual Phase Approach

The first approach demodulates the returned pulse with a cosine and a sine waveform. This would be the same as transmitting a cosine and a sine signal and demodulating them both with a cosine. The result is an in-phase and quadrature measurement.

$$\begin{aligned} R(\omega) &= \frac{1}{N} \sum_{i=1}^N r(t_i) \cos(\omega t_i - \theta) & R(\omega) &= \frac{a_0}{2} + \frac{a_1}{2} \cos(\phi) \\ Q(\omega) &= \frac{1}{N} \sum_{i=1}^N r(t_i) \sin(\omega t_i - \theta) & Q(\omega) &= \frac{a_1}{2} \sin(\phi) \end{aligned}$$

**Equations 3.2**

Equations 3.2 show the processing steps and the final scalar values. It is assumed that the sampling rate is sufficiently high to prevent aliasing. Note that all the unknown parameters appear in these scalar measurements. A separate measurement must be made at each frequency used in the imaging system.

A significant issue exists in the in-phase value. The  $a_0$  term is the reflection coefficient of the wall surface. This value must be determined prior to the application of this dual phase method. This is the so-called ‘‘layer peeling’’. The wall surface must be determined, then the inner wall structure, then the imaging of the area behind the wall. Here we focus only on the solving of the middle problem – the inner wall structure. With the removal of the  $a_0$  value, the in-phase measurement becomes what is shown in Equation 3.3

$$R(\omega) - \frac{a_0}{2} \rightarrow R(\omega) = \frac{a_1}{2} \cos(\phi) \quad \text{Equation 3.3}$$

Now the form of the in-phase and quadrature values can be divided to remove  $a_1$  (unknown). The result is a tangent of the unknown phase. By taking an arctangent, the desired value is reached. Equation 3.4 shows the final form. Note that the R and Q values must be measured at each frequency and Equation 3.4 applied. This gives an estimated wall phase value at every required frequency.

$$\hat{\phi}(\omega) = \arctan\left(\frac{Q(\omega)}{R(\omega)}\right) \quad \text{Equation 3.4}$$

Figure 3.1 shows the estimated phase for the three point scatterer simulation. The red line is the actual phase value at each frequency. The phase is linear because the wall in this simulation is homogeneous and non-dispersive. The phase ramp is due to the linearly increasing frequency. The advantage of this approach is that, were the wall dispersive (meaning that the phase changed non-linearly in frequency), the required phase at each frequency would be sufficiently determined.

The blue wrapping phase is the estimated value. The wrapping occurs because the range of the arctangent function cannot determine the phase outside of the  $-\pi$  to  $\pi$  interval. However, mathematically, it is not necessary to determine the true phase. Only the value within

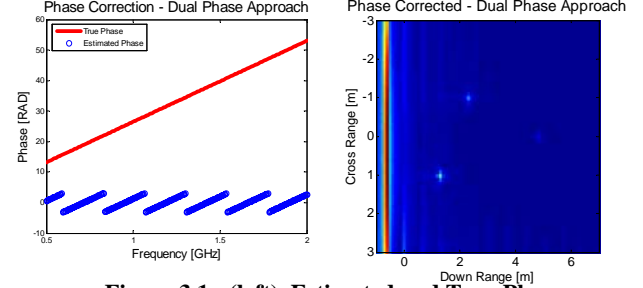


**Figure 3.1: (left) Estimated and True Phase (right) Image After Correction with Dual Phase Approach**

this range is required to affect the necessary phase corrections in the image processor. Figure 3.2 shows the resulting image after the correction. Note that the three points have been successfully focused.

### 3.2 Dual Frequency Approach

The dual phase approach makes an assumption that may not be practically achievable. This is the assumption that the return from the front of the wall has been removed (i.e. canceled). Because of this a second approach is introduced here. Some assumptions must also be made for this method. Two frequencies will be used to generate a set of non-linear equations that will be solved iteratively using a non-linear, successive approximation method. The assumptions here are that the reflection coefficients remain constant for the two frequencies. Since these values are slowly varying in frequency, this assumption is very nearly true. As long as the frequencies do not get too far apart, this assumption will hold.

Our starting point is with the quadrature measurements R and Q at two frequencies  $f_1$  and  $f_2$ . The reason for using quadrature is that the  $a_0$  unknown is naturally removed during the demodulation process. If we also consider the in-phase measurements, we have to solve for the added  $a_0$  unknown. Since  $a_0$  and  $a_1$  are nuisance parameters, we utilize only  $q_1$  and  $q_2$ . The expressions for these measurements are given by Equation 3.5. These are rewritten in the form of functions  $F_1, F_2$  for use in the Jacobian matrix described next.

$$\begin{aligned} q_1 &= \frac{a_1}{2} \sin(\phi_1) & F_1(x) &= \frac{x_1}{2} \sin\left(\frac{4\pi f_1}{c} x_2\right) \\ q_2 &= \frac{a_1}{2} \sin(\phi_2) & F_2(x) &= \frac{x_1}{2} \sin\left(\frac{4\pi f_2}{c} x_2\right) \end{aligned}$$

**Equations 3.5**

$$J = \begin{bmatrix} \frac{\partial F_1(x)}{\partial x_1} & \frac{\partial F_1(x)}{\partial x_2} \\ \frac{\partial F_2(x)}{\partial x_1} & \frac{\partial F_2(x)}{\partial x_2} \end{bmatrix} = \begin{bmatrix} \frac{1}{2} \sin\left(\frac{4\pi f_1}{c} x_2\right) & \frac{x_1}{2} \sin\left(\frac{4\pi f_1}{c} x_2\right) \frac{4\pi f_1}{c} \\ \frac{1}{2} \sin\left(\frac{4\pi f_2}{c} x_2\right) & \frac{x_1}{2} \sin\left(\frac{4\pi f_2}{c} x_2\right) \frac{4\pi f_2}{c} \end{bmatrix}$$

**Equations 3.6**

The parameter  $x_1$  is the reflection coefficient from the back of the wall. The parameter  $x_2$  is the thickness-permittivity-square-root product. The  $x_2$  parameter is of primary interest. Knowledge of this value allows for the phase distortion to be corrected.

Define the two element vectors  $q$  and  $F$  by contacting the two respective terms in Eq 3.5. The problem of estimating the parameters  $x_1$  and  $x_2$  can be formulated as a non-linear least squares problem,  $\min_x (|q-F(x)|^2)$ , equivalent to maximum likelihood under an additive Gaussian noise model  $q=F(x)+\text{noise}$ . Starting with an initial value of  $x_1, x_2$ , we can find the least squares solution using the iterative Newton-Raphson approach. This algorithm uses successive approximations to iterate to a solution. The Jacobian matrix shown in Equation 3.6 is determined using the non-linear equations  $F_1, F_2$ .

The Jacobian matrix defines a hyper-plane that is tangent to the manifold of the  $F_1, F_2$  functions at the point of the current estimates of  $x_1, x_2$ . A solution to the equations is found within this plane and this solution will be closer to the true answer than the previous estimates. The same is true for the next solution until the estimates no longer change. This is the successive approximation strategy. Mathematically, this can be written as in Equations 3.7.

$$\hat{x}_k = \hat{x}_{k-1} + (J_{k-1}^T J_{k-1})^{-1} J_{k-1}^T (q - F(\hat{x}_{k-1}))$$

$$q = \begin{bmatrix} q_1 \\ q_2 \end{bmatrix} \quad x = \begin{bmatrix} x_1 \\ x_2 \end{bmatrix} \quad F(x) = \begin{bmatrix} F_1(x) \\ F_2(x) \end{bmatrix}$$

Equations 3.7

A logical starting point is to choose the initial values of  $x_1, x_2$  to determined by the values we expect (i.e. the mean values) for the wall being interrogated. This incorporates the a priori information we have about the wall. For this simulation only a few iterations are required for the estimates to converge. Figure 3.3 shows the convergence in the  $x_1$  parameter while Figure 3.4 shows the same for  $x_2$ . The starting values were 0.8 for  $x_1$  and 0.6 for  $x_2$ . The actual values were 1.0 and 0.6325 respectively. The estimated values reached by the algorithm were 1.3 and 0.6270.

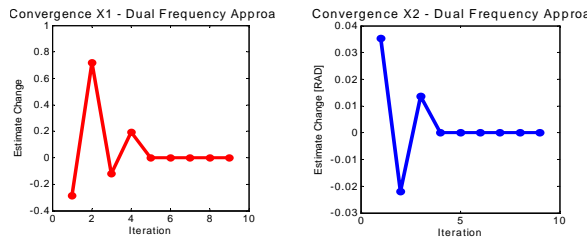


Figure 3.3 Convergence of Parameters  $x_1$  and  $x_2$

The  $x_2$  parameter corresponds to the  $\tau\sqrt{\epsilon_2}$  product, which is the key element in the unknown phase experienced by the waves traveling through the wall. Once this parameter is estimated, the image can be phase corrected at any frequency. So, provided that the wall structure does not change, only one sounding has to be made in the

dual frequency approach. The resulting image is shown in Figure 3.5.

Note that the 3 point scatterers are well focused in Figure 3.5. The dual frequency method shows much promise. Unfortunately, it does have challenges to be addressed in future work, namely local minima of the objective function  $\|q-F(x)\|^2$ .

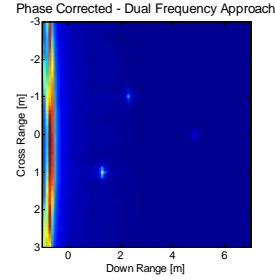


Figure 3.5: Image after correction with the Dual Frequency approach.

#### 4. CONCLUSIONS

Two approaches have been proposed for determining the unknown phase produced by plane waves propagating through a wall. It has been shown that this unknown phase prevents proper imaging of the scene behind the wall using a See-Through-The-Wall radar. Both approaches were effective in determining and removing the unknown phase when their underlying assumptions were satisfied.

The two approaches were also quite robust when contaminated with noise. Both functioned well at a signal-to-noise (SNR) of -10dB. (SNR here is defined as the mean squared amplitude of transmitted sinusoid to the variance of the noise.) This robustness is due to the correlating of the return signal with the transmit signal. Each pulse was sampled in such a way that 1000 points were collected. When all these samples are correlated with the signal and averaged together, a reduction in noise variance of a 1000 is affected.

- [1] Cafforio, C., Prati, C., Rocca, F., "SAR Data Focusing Using Seismic Migration Techniques," *IEEE Transactions on Aerospace and Electronic Systems*, Vol. 27, No. 2, March 1991, pp. 194-206.
- [2] Gray, S.H., "Speed and Accuracy of Seismic Migration Methods," Technical Report: Amoco Exploration and Production Technology.
- [3] Jakubowicz, H., Levin, S., "A Simple Exact method of 3-D Migration," *Geophysical Prospecting*, Vol. 31, pp. 1-33.
- [4] Carrara, W., Goodman, R., Majewski, R. *Spotlight Synthetic Aperture Radar*. Artech House: Boston. 1995.
- [5] Yu, Y.J., Yu, T.J., Carin, L., "3D Inverse Scattering of a Dielectric Target Embedded in a Lossy Half-Space," *IEEE Transactions on Geoscience and Remote Sensing*, Vol. 42, No. 5, May 2004, pp. 957-973.